'Too cold' bottom layers at the base of the Scotian Rise

by Georges L. Weatherly[1] and Edward A. Kelley, Jr.[1]

ABSTRACT

CTD data indicate that the bottom boundary layer in a region of the western North Atlantic near 40N 62W is a distinct body of relatively cold (θ < 1.82°C), fresh (S < 34.894‰) water. This region is a strip ~ 100 km wide aligned approximately along isobaths centered near the 4900 m isobath on the continental margin near its base. This bottom layer has a thickness ~ 60 m and it is capped by a transition region of comparable thickness. Examination of other data suggests that this distinct bottom layer is part of a continuous ribbon or filament found on the continental margin near its base extending eastward from the region to about 50W and at least westward to about 72W. Current meter records indicate that this 'Cold Filament' flows equatorward embedded in the overlying fluid at an average rate of ~ 9 cm/s.

1. Introduction

In examining near-bottom CTD data obtained in September-October 1979 on the continental rise south of Nova Scotia we found two unexpected results. The first was the presence of a distinct body of relatively cold water lying on the continental rise near its base having a width about 100 km and a thickness about 60 m. Examination of historical data together with other observations reported here suggests that what was observed is part of a thin, long (order 10^3 km) ribbon or filament of relatively cold, fresh water flowing over the bottom on the continental rise near its base. Hereafter, we refer to this feature as the Cold Filament.

The 1979 CTD data were taken as part of the site selection and characterization phase of the High Energy Benthic Boundary Layer Experiments (HEBBLE) program (Hollister *et al.*, 1980). HEBBLE is a project for studying the deep ocean bottom boundary layer in a region where the currents are thought to be strong enough to put sediments into suspension. The second unexpected result has to do with bottom boundary layers in the surveyed region. In a portion of the so-called HEBBLE area (Fig. 1) the bottom boundary layer was found to be a distinct body of cold water. That is, in the Cold Filament the bottom boundary layer *is* the Cold Filament.

The purpose of this paper is to present some results of the 1979 CTD study in the HEBBLE area which pertain to the Cold Filament and to present subsequently

1. Department of Oceanography, Florida State University, Tallahassee, Florida 32306, U.S.A.

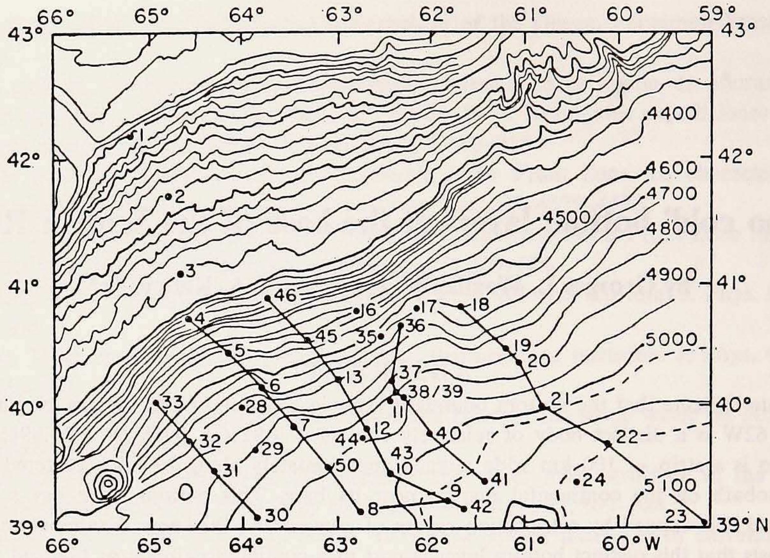

Figure 1. Bathymetric map of HEBBLE area. *Knorr* 74 CTD stations are indicated. Solid lines connecting CTD Stations are transects shown in Figures 2 and 4. Depths in meters.

obtained observations which were prompted by the 1979 CTD survey result. In Part 2 CTD and optical transmissivity data obtained in the HEBBLE area in 1979 are presented. In Part 3 similar data obtained a year later are presented. Current meter observations made in the same area are considered in Part 4. Part 5 is a summary and discussion.

2. September-October 1979 (*Knorr* 74) CTD/transmissometer data

Shown in Figure 1 are the locations of 43 full water column CTD casts hydrographic stations made between 9 September 1979 and 1 October 1979 as part of the HEBBLE program. The data were obtained on R/V *Knorr* Cruise 74 by the Optical Oceanography Group at Oregon State University using a Neil Brown Instrument System CTD. The data were processed by that Group and made available to us in computer print-out form.

Attached to the CTD was an optical transmissometer. The transmissivity data and temperature data are discussed in Spinrad (1982) and Pak and Zaneveld (1982). The results presented here complement the later study. Our original objectives in examining the *Knorr* 74 hydrographic data were to provide information necessary for initializing a numerical bottom boundary layer we wanted to apply to the HEBBLE area (e.g., Weatherly and Martin, 1978) and to assemble a set of bottom layer (BL) observations for comparison to model predictions. A study of another bottom boundary layer over a continental margin (Weatherly and Martin, 1978) showed the importance of knowing the background mesoscale hydrographic field

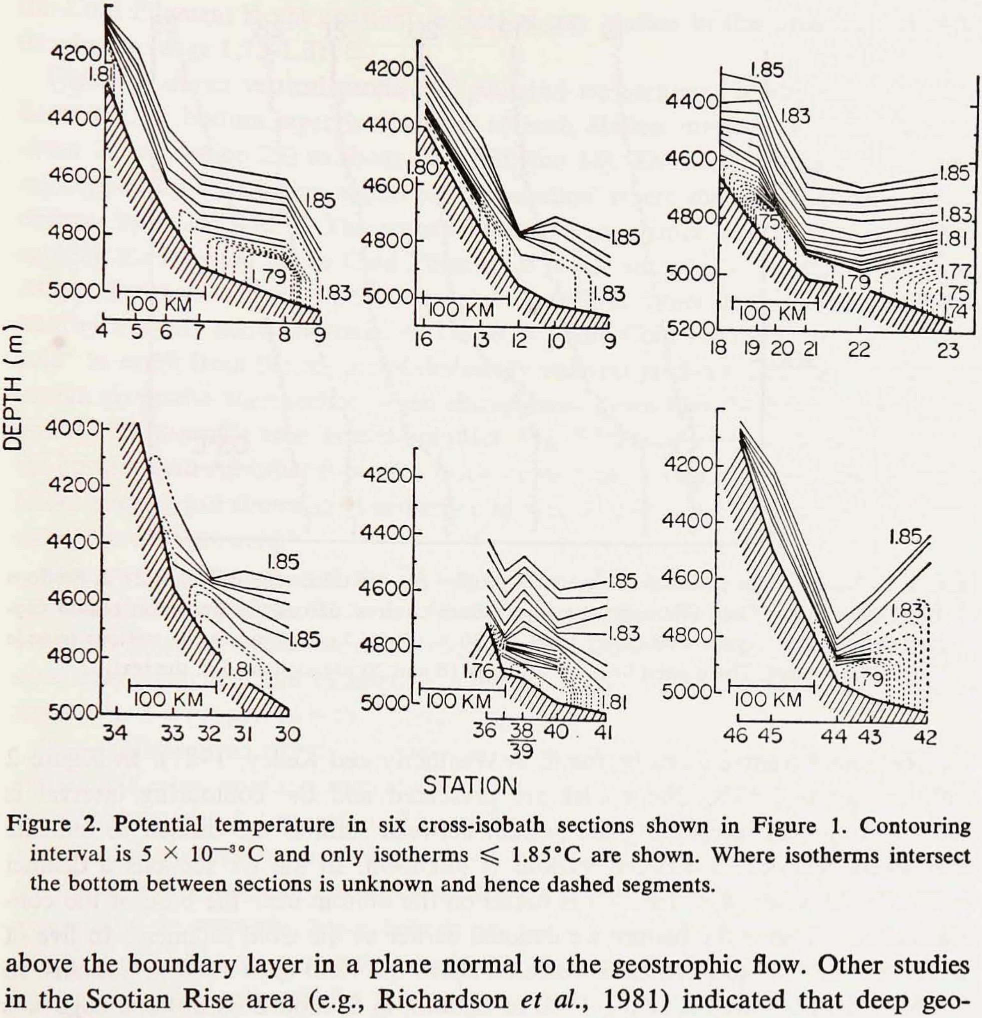

Figure 2. Potential temperature in six cross-isobath sections shown in Figure 1. Contouring interval is 5 × 10⁻³°C and only isotherms ⩽ 1.85°C are shown. Where isotherms intersect the bottom between sections is unknown and hence dashed segments.

above the boundary layer in a plane normal to the geostrophic flow. Other studies in the Scotian Rise area (e.g., Richardson *et al.*, 1981) indicated that deep geostrophic currents there are aligned approximately along isobaths. Thus we decided to examine hydrographic transects normal to isobaths in the HEBBLE area.

During the approximate three week time of the *Knorr* 74 cruise near-bottom currents varied from about 10-40 cm/s (Bird *et al.*, 1982; Richardson *et al.*, 1981). Thus water parcels moved distances order tens of kilometers per day. To obtain more synoptic information we considered sections completed in several days time. Six sections (elapsed time in parentheses) were examined: (1) Stations 4-9 (2 days, 6 hours), (2) Stations 9, 10, 12, 13, 16 (3 days, 15 hours), (3) Stations 18-23 (2 days, 15 hours), (4) Stations 30-34 (1 day, 21 hours), (5) Stations 36-41 (2 days, 3 hours) and (6) Stations 42-46 (2 days, 4 hours). These sections are indicated in Figure 1; notice that Section 6 is nearly a repeat of Section 2.

Near-bottom potential temperature θ is contoured for each section in Figure 2

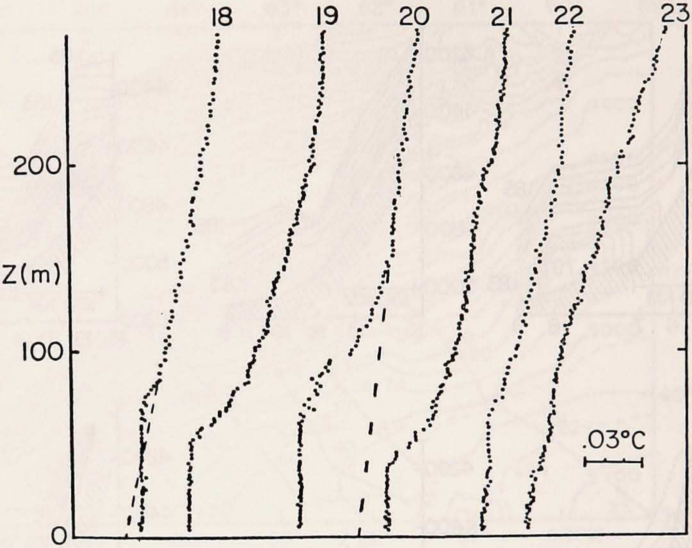

Figure 3. Near-bottom potential temperature profiles for the third section in Figure 2. Stations 19-21 were in the Cold Filament; the temperature contrast across the transition region capping their bottom layers is relatively large ($\sim 30 \times 10^{-3}$°C) compared to the stations outside the Cold Filament. The dashed lines for Stations 18 and 20 are explained in the text.

(full column θ transects can be found in Weatherly and Kelley, 1981). In Figure 2 only isotherms 1.85°C and colder are presented and the contouring interval is .005°C. Contours intersecting the bottom between stations are dashed to indicate that where this occurs between stations is unknown. In the six sections a distinct body of cold water ($\theta < 1.82$°C) is found on the bottom near the base of the continental rise. This is the feature we denoted earlier as the Cold Filament. In five of the transects the Cold Filament is centered about the 4850 m to 5000 m isobaths. In Section 2 it is centered near the 4500 m isobath; in Section 2 its upslope edge was not sampled.

Before continuing we comment on three other features apparent in Figure 2. First, Section 3 extends furthest out onto the Sohm Abyssal Plain and on this section another distinct body of cold water on the abyssal plain is seen. Such a feature is seen often in other hydrographic sections extending onto the abyssal plain in this area (e.g., McCartney *et al.*, 1980, Figure 3). We do not consider this feature any more in this paper. Second, Section 1 shows a cold bottom layer centered near Station 4 which did not extend up to Station 3 (Weatherly and Kelley, 1981). This may be an upslope protrusion of the Cold Filament. Third, the core potential temperature of the Cold Filament core increases from about 1.75°C to 1.81°C going from east to west. Based on other data to be presented later, we do not think this is a permanent feature but rather a reflection that the core potential temperature of the Cold Filament is not constant in time at any section in this area but varies in time in the range 1.75-1.81°C.

Figure 3 shows vertical profiles of potential temperatures at the Stations along Section 3. A bottom layer is apparent at each Station ranging in thickness from about 20 m (Station 23) to about 70 m (Station 18). The BLs in the Cold Filament are capped by a transition region or 'thermocline' where the potential temperature changes by about .030°C. The potential temperature change across the 'thermocline' capping the BLs not in the Cold Filament is about an order of magnitude smaller. Above the 'thermocline' at all stations the θ-profile is rather uniform and characterized by a nearly constant gradient. The BLs in the Cold Filament are clearly "too cold" to result from the mixing of the nearly uniform gradient; i.e., the temperature profile above the 'thermocline' when extrapolated down into the BL does not intersect the BL θ-profile near its mid-point (cf. Fig. 3 Stations 18 and 20) but intersects the bottom first. All other θ-profiles made in the Cold Filament in the other sections (these profiles are shown in Weatherly and Kelley, 1981) show BLs which without exception are "too cold."

Of more significance than the BLs in the Cold Filament being "too cold" is that in the Cold Filament the BL *is* the Cold Filament. The BL in the Cold Filament is a distinct body of colder water. Later, using subsequently obtained CTD data, we show that while the Cold Filament is a distinct body of colder water it is not anomalous in its θ-S properties with the overlying water.

The optical transmissivity per meter of the water for the six sections is shown in Figure 4. Lower numbers indicate murkier water. A clear visual correlation with the corresponding θ transects in Figure 3 is not evident. Only Sections 3, 4, 5, 6 show a core of murkier water roughly coincident with the core of the Cold Filament. As noted earlier, near-bottom velocities in the area during the *Knorr* 74 cruise varied appreciably in strength. Since bottom sediments may go into suspension during intervals of strong flows thereby markedly changing the transmissivity, and near-bottom flows can vary over the time interval a section was made, there is no *a priori* reason to expect the sections in Figure 4 to correlate visually with those in Figure 3. From Figure 4 one sees that, as noted in Pak and Zaneveld (1982), the near-bottom water tends to be murkier near the base of the rise. Only in the sense that the Cold Filament is also found near the base of the rise is there a correlation in the *Knorr* 74 transmissivity transect data and the Cold Filament.

3. September 1980 (*Knorr* 83) CTD/transmissometer data

In September 1980 we returned to the area on R/V *Knorr* Cruise 83 and obtained further CTD/transmissometer profile data. Our purposes in obtaining additional data were to see if the Cold Filament was again present, and if so, to obtain salinity data of better quality than the *Knorr* 74 data to determine whether or not its θ-S properties were anomalous.

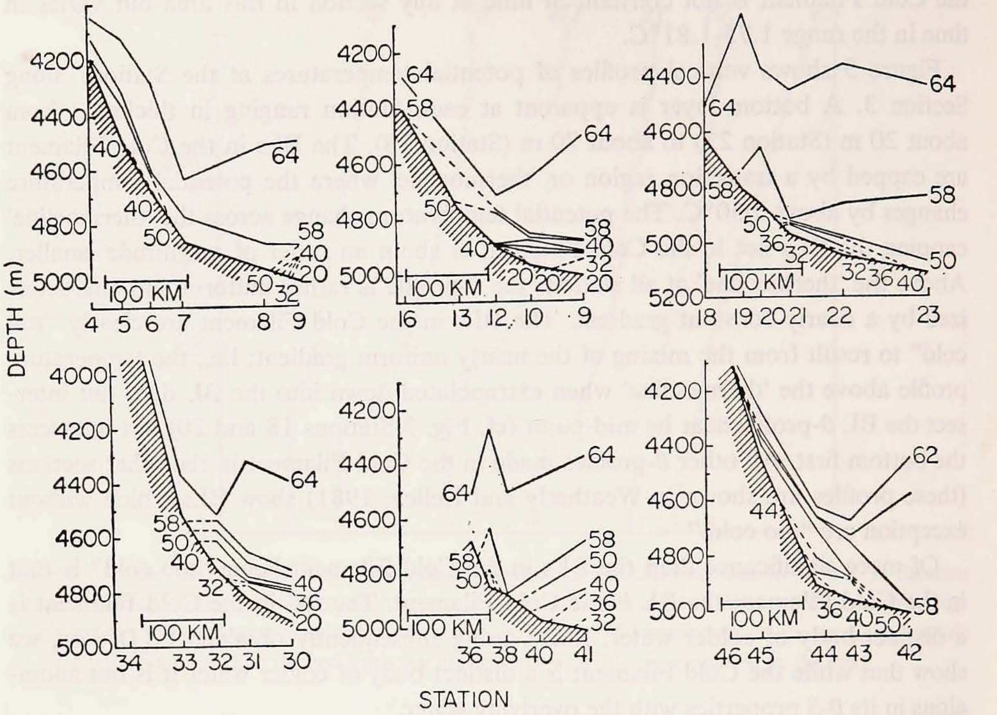

Figure 4. Optical transmissivity per meter path length transects corresponding to the θ-sections shown in Figure 2. While the water tends to be murkier (lower transmissivity values) near the base of the rise, there is little visual correlation with the Cold Filament (Fig. 2).

The location of the 22 stations made during the *Knorr* 83 cruise are shown in Figure 5. The observations were made with a Neil Brown Instrument System CTD from and operated by the University of Rhode Island. Attached to the CTD was an optical transmissometer provided by the Optical Oceanography Group at Oregon State University. The data were processed by the CTD Group at the Woods Hole Oceanographic Institution and made available to us in 2 db intervals. More details are available in Weatherly *et al.* (1981).

Two near-bottom transects of θ and transmissivity, Section A (Stations 5-10, total elapsed time 2 days, 18 hours) and Section B—obtained a week later—(Stations 15-22, total elapsed time 3 days, 15 hours) are shown in Figures 6 and 7. The Cold Filament is evident in both θ sections. Its location on the rise and its width and thickness are similar to that seen in Figure 2. The transmissivity transect for Section A in Figure 6 indicates that the Cold Filament was relatively murky. The comparable transect for Section B in Figure 7 indicates also that the Cold Filament was also relatively murky. Section B shows two murky cores flanking the cold core as do some of the sections in Figure 4. However, the one seen above Station 20

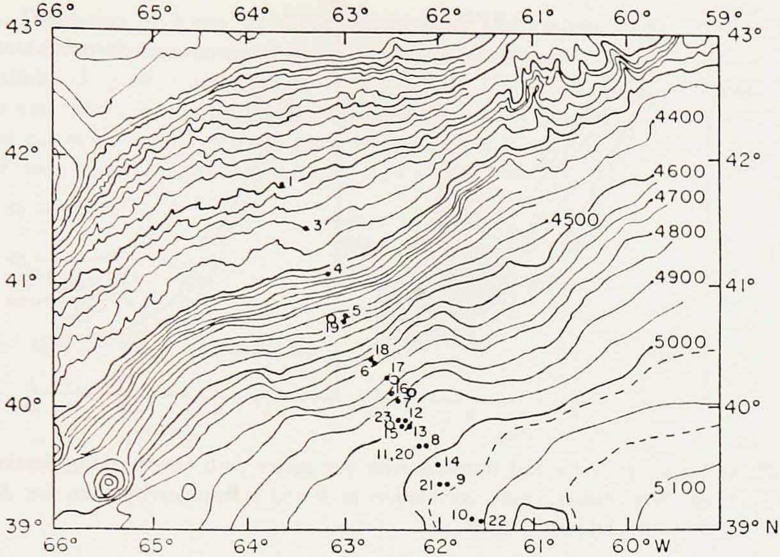

Figure 5. As Figure 1 except CTD stations from the *Knorr* 83 cruise are now indicated by solid, numbered dots. Open circles near CTD stations 23, 17, and 19 indicate the Deep, Middle, and Shallow Moorings, respectively.

may not be significant. The near-bottom transmissivity at Stations 15 and 20 differed by 2% (Table 1) and transmissivity in the BLs at both stations varied by more than 2% (Fig. 9). If a value averaged across the BL rather than the observed near-bottom values had been used for contouring purposes in Figure 7, the second murky core centered about Station 20 would not appear. However, the other murky core centered above Station 16 would still remain centered at this station. In Section B the murkiest water is slightly upslope of cold core centered above Station 15. This raises the question: if transmissivity data had been available for Station 7 in Section A would the murky core be found slightly upslope of the cold core for this section as well?[2]

Near-bottom profiles of θ, salinity S, transmissivity, and σ_5 for one of the stations in the Cold Filament, Station 14, are shown in Figure 8 (similar profiles for all stations are in Weatherly *et al.*, 1981). From the S and σ_5 profiles in Figure 8 it is apparent that, in the sense discussed earlier that the BL in the Cold Filament is "too cold," this BL is "too fresh" and "too dense." Examination of similar figures in Weatherly *et al.* (1981) for stations in the Cold Filament—these stations are indicated in Table 1—show that the BLs in the Cold Filament are all "too fresh" and

2. Footnote added in proof. A recent manuscript by I. N. McCave has a figure showing contours of suspended particle concentrations along Section A determined from Coulter counter analysis of water samples. A maximum bottom layer concentration at Station 7 is indicated, i.e., the murkiest water is upslope of the cold core.

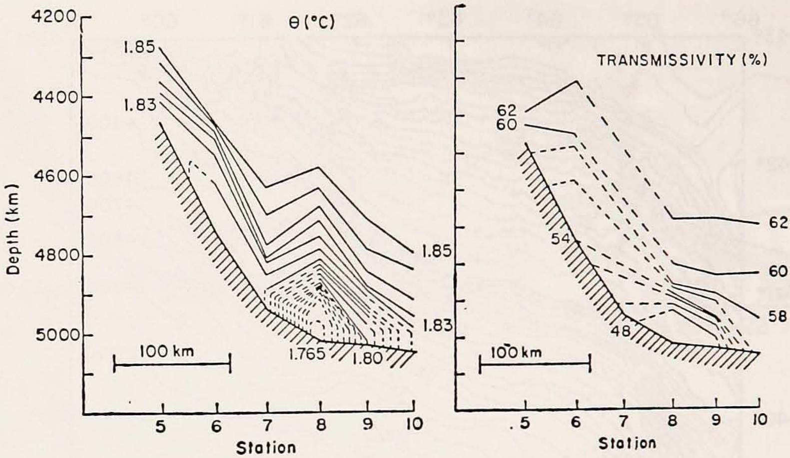

Figure 6. Potential temperature and transmissivity per meter path length along Section A for *Knorr* 83 cruise. Note closer visual correlation in θ and transmissivity than for *Knorr* 74 data. No transmissivity data for Station 7.

"too dense." Below we present results which show that, as in the *Knorr* 74 data, the BLs in the Cold Filament seen in the *Knorr* 83 data are all "too cold."

In the BL in Figure 8 ($z < 70$ m) θ, *S* and transmissivity are nearly homogeneous. The BL thickness determined by either the θ, *S* or transmissivity profiles is essentially the same and is about 70 m. Pak and Zaneveld (1982) in discussing data obtained during *Knorr* 74 make a distinction between a BL determined from the θ profile—which they call a bottom mixed layer—and a BL determined from the transmissivity profile—which they call a homogeneous bottom nepheloid layer. They find the latter to be about 20% thicker than the former (their Fig. 2). In Figure 9

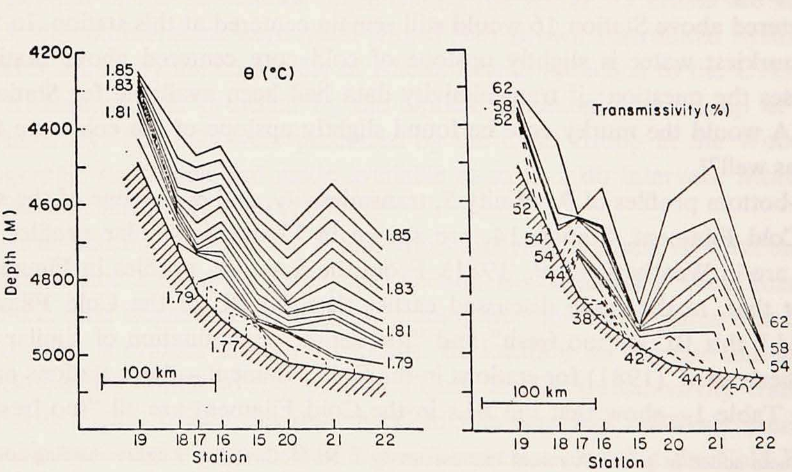

Figure 7. As for Figure 6 except Section B for *Knorr* 83 cruise. Double murky core is discussed in text.

Table 1. Tabulation of *Knorr* 83 CTD bottom layer and bottom layer cap results. The BL thickness inferred from potential temperature (θ), transmissivity per meter path length (*TR*) and salinity (*S*) profiles are given by h_θ, h_{TR} and h_S. The thickness of the thermocline, nephelcline and halocline capping the bottom layer are inferred from θ, *TR* and *S* profiles. Near-bottom values of θ, *TR* and *S* are given in last three columns. A "*" denotes a station in the Cold Filament, a "—", no data, and a "?", not evident from the data.

St.	Depth (m)	h_θ (m)	h_{TR} (m)	h_s (m)	Thermo-cline thickness (m)	Nephel-cline thickness (m)	Halocline thickness (m)	θ_o (°C)	*TR* (%)	$(S_o - 34)$ ‰
1	3041	68	—	70	110	—	110	2.451	—	.931
3	3562	66	63	75	20	20	20	2.026	65	.914
4	4087	38	35	34	10	10	10	1.853	62	.903
5	4472	67	60	64	15	20	15	1.827	57	.894
6	4748	110	?	?	20	?	?	1.821	53	.891
7	4976	53	—	142	20	—	?	1.819	—	.894
8*	5025	104	93	106	105	105	105	1.766	47	.884
9*	5038	73	76	82	75	75	75	1.800	48	.891
10	5056	57	70	85	50	55	?	1.828	57	.894
11	5020	?	50	39	?	30	30	1.807	46	.899
12*	4981	56	54	59	150	150	6	1.765	50	.887
13*	4985	60	30	54	5	35	5	1.784	16	.892
14*	5030	68	64	69	80	80	80	1.767	45	.886
15*	4981	50	40	53	25	25	25	1.768	46	.891
16*	4913	55	52	60	250	250	250	1.777	37	.888
17*	4841	102	103	89	110	110	110	1.790	42	.891
18*	4725	55	52	65	110	125	100	1.796	55	.892
19	4494	132	127	136	80	80	70	1.804	50	.893
20*	5024	76	72	76	100	100	100	1.775	44	.886
21*	5042	26	35	32	200	200	200	1.781	46	.888
22	5065	72	72	77	25	25	25	1.791	54	.891
23*	4973	37	33	35	100	100	100	1.780	47	.893

are near-bottom θ and transmissivity profiles for all stations (because of instrument problems no transmissivity profiles were obtained for Stations 1 and 7). Thickness of the BLs determined separately from the θ and transmissivity profiles are listed in Table 1. In contrast to Pak and Zaneveld we find the thickness of the BL determined from θ and transmissivity profiles to be about the same. Also listed in Table 1 are thicknesses of the BL determined from *S* profiles in Weatherly *et al.* (1981). Because the *S* contrast above the BL is often marginally detectable with the CTD used, especially for stations not in the Cold Filament, BL thicknesses inferred from *S* profiles have greater uncertainty. However, to within instrumental resolutions, BL thicknesses determined from *S* profiles agree with those inferred from θ and transmissivity profiles.

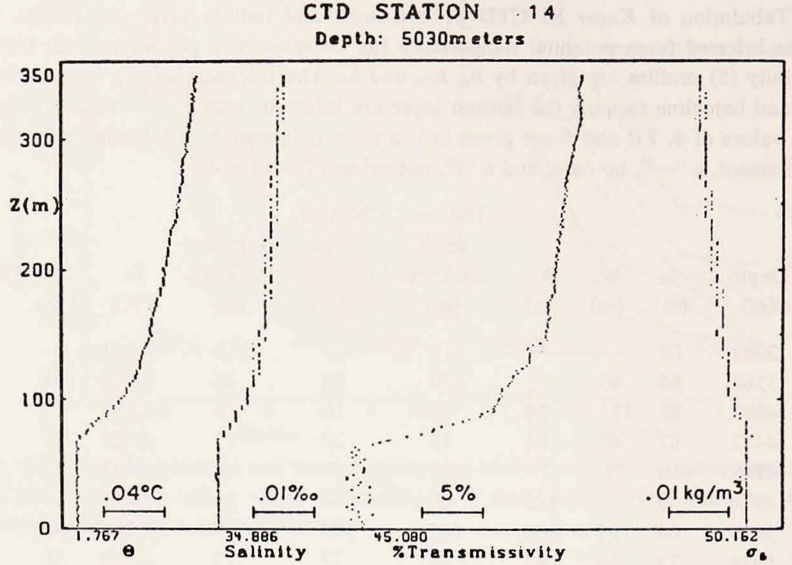

Figure 8. Near-bottom profiles of θ, salinity, transmissivity and σ_5 for one of the *Knorr* 83 stations (Station 14) in the Cold Filament.

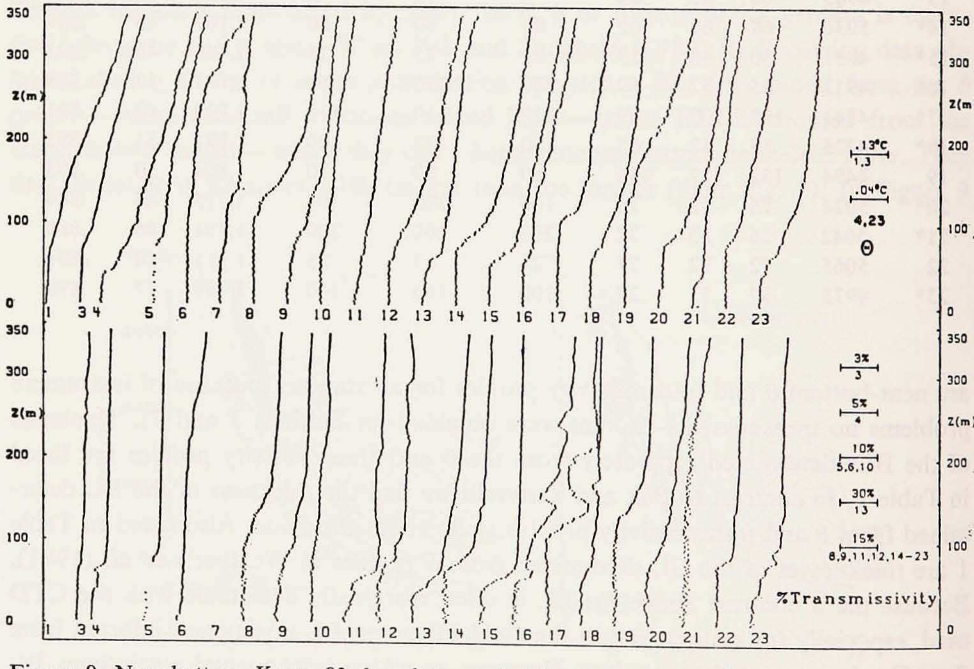

Figure 9. Near-bottom *Knorr* 83 θ and transmissivity per meter path length profiles. Numbers under profiles indicate station. Near-bottom values of θ and transmissivity are listed in Table 1.

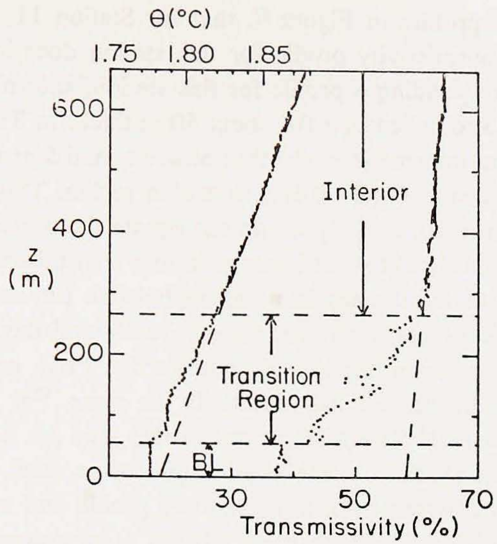

Figure 10. Profiles for *Knorr* 83 CTD Station 16 re-drawn with longer vertical scale.

Although the BL is often essentially homogeneous (to within 10^{-3}°C in θ and 3% in transmissivity) as in Figure 8, there are cases where a BL is evident but it is clearly not homogeneous in θ and/or transmissivity (e.g., Station 13 in Fig. 9). For this reason we have designated these layers as bottom layers (BLs) rather than bottom mixed layers.

From Figures 6 and 7 it is apparent that Stations 8, 9, 15, 16, 17, 18, 20, 21 extend into the Cold Filament. From Figure 9 it is also apparent that, as discussed earlier, the BLs for all these stations except 16 are "too cold." From Figure 9 it appears that the BL for Station 16 could be due to mixing of a uniform interior gradient. The θ and transmissivity profiles for Station 16 are redrawn with an expanded vertical scale in Figure 10. It is apparent from examining these profiles that the transition region capping the BL is very thick. Thus with the expanded vertical scale the BL for Station 16, like all others in the Cold Filament, is clearly "too cold." Finally, since the BLs at Stations 12, 13, 14, and 23 were "too cold" and colder than 1.82°C we infer that these stations also extended into the Cold Filament.

The average thickness of the BLs in the Cold Filament is 64 m and out, it is 81 m. For comparison, the *Knorr* 74 data obtained a year earlier gives an average BL thickness in the Cold Filament of 63 m and out of the Cold Filament, 76 m. To compute these latter values we used near-bottom θ profiles in Weatherly and Kelley (1981). Thus both the *Knorr* 74 and 83 data yield average BL thicknesses in the Cold Filament of about 60 m and average BL thicknesses out of the Cold Filament about 15 m thicker.

Only one of the θ profiles in Figure 9, that for Station 11, shows no apparent BL. However, the transmissivity profile for this station does indicate a BL about 50 m thick. The corresponding S profile for this station, shown in Weatherly *et al.* (1981) but not here, also indicates a BL about 50 m thick. In Table 1 the BL thickness for Station 11 was inferred from the transmissivity and S profile.

Capping the BLs seen in Figure 9 is a transition region. This region is indicated for one station in Figure 10. Initially we do not equate the transition region inferred from a θ profile (thermocline) to that inferred from a transmissometer profile (nephelcline). Thicknesses of the thermocline and nephelcline for each station are listed in Table 1. These thicknesses were determined visually and therefore are somewhat subjective. Nonetheless, some features are noteworthy. First, generally the thermocline and nephelcline thicknesses are essentially the same. For a few stations, e.g., Station 12, they differ or if discernible in one profile they are not clearly evident in the other, e.g., Station 11. Since some physical processes, such as settling velocities of suspended matter, determine the transmissivity profile and not necessarily the θ profile, it is not surprising that there is not always a one-to-one correspondence in these profiles at all stations. However, since the thermocline and nephelcline are usually of the same thickness in the *Knorr* 83 data we will generally denote the thermocline and nephelcline as the transition region or BL cap. Second, at any one station the transition region thickness is usually comparable in thickness to that of the BL. The transition region for Station 16, Figures 9 and 10, is about three times thicker than the BL and is the thickest for any station we have examined in the HEBBLE area. Third, a comparison of the transition region thickness for stations in and out of the Cold Filament—see Table 1—shows that the transition region is generally thicker above BLs in the Cold Filament. The average transition region thickness for stations in the Cold Filament is about 100 m while for those out of the Cold Filament it is about 40 m. Possible explanations for thicker transition regions above the Cold Filament are considered later. Comparably thicker thermoclines above the Cold Filament are also apparent in the *Knorr* 74 data (e.g., Fig. 3).

In Figure 11 are θ-S plots for two stations out of the Cold Filament (Stations 7, 10) and two stations in the Cold Filament (Stations 8, 9). The '( )' in this figure bracket values for the so-called Worthington-Metcalf line for the North American Basin (Wright and Worthington, 1970); the dashed line, shown only for $\theta < 2°C$, is the average θ-S curve for the Labrador Basin *(ibid).* All values in Figure 11 with $\theta < 1.81°C$ are from the Cold Filament. We see from Figure 11 that the θ-S properties for the Cold Filament are representative for the North American Basin. The Cold Filament does not appear to be a ribbon of Labrador Basin deep water.

4. Current meter observations

Our intent here is to present some current meter velocity and temperature ob-

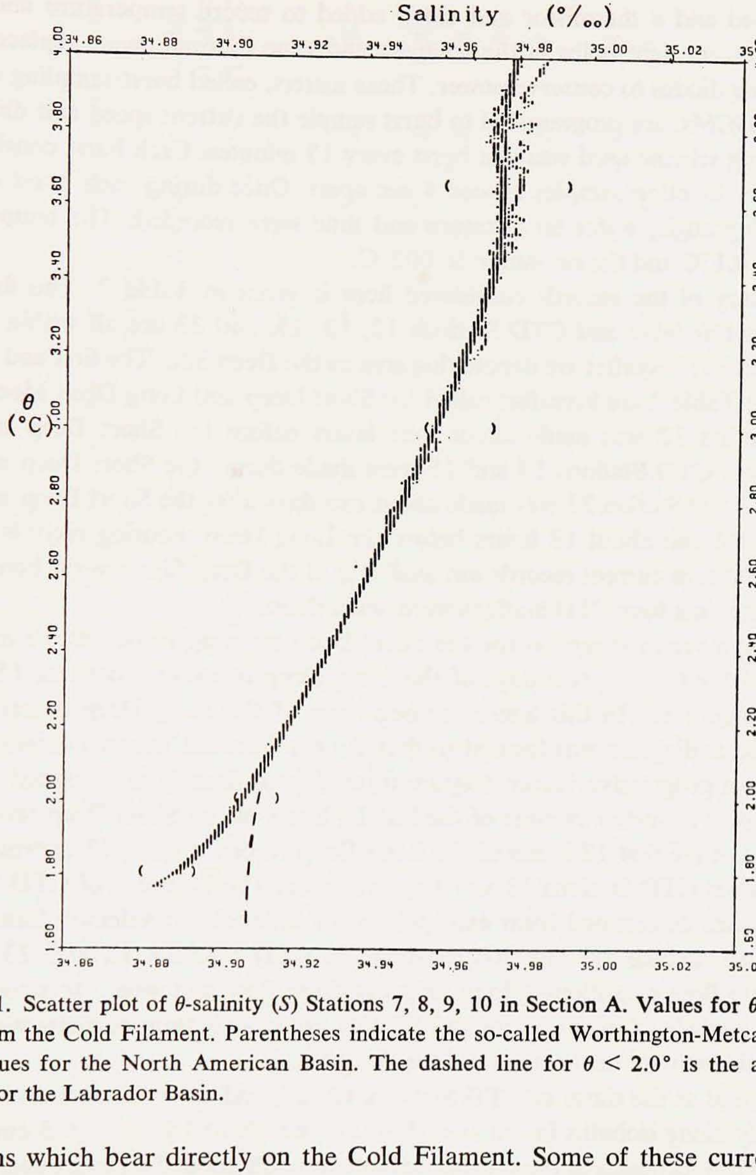

Figure 11. Scatter plot of θ-salinity (S) Stations 7, 8, 9, 10 in Section A. Values for $\theta \leqslant 1.82$°C are from the Cold Filament. Parentheses indicate the so-called Worthington-Metcalf bracketing values for the North American Basin. The dashed line for $\theta < 2.0$° is the average θ-S curve for the Labrador Basin.

servations which bear directly on the Cold Filament. Some of these current meter records are considered briefly in another context in Kelley *et al.* (1982). The current meters used have not been previously described and before presenting their data we give a brief description of them. They are Geodyne 101-1 film recording meters (EG & G, Waltham, Massachusetts) which were converted at Florida State University to magnetic tape cassette recordings using Sea Data (Sea Data Corporation, Newton, Massachusetts) cassettes and circuit boards. The Geodyne 101-1 is essentially a film recording version of the Geodyne 850 current meter. The inclinometers were retained and a thermistor and clock added to record temperature and time. The incandescent light bulbs in the compass and vane followers were replaced with light-emitting diodes to conserve power. These meters, called burst-sampling current meters or BSCMs, are programmed to burst sample the current speed and direction. The sampling scheme used was one burst every 15 minutes. Each burst consisted of 8 speed and direction samples spaced 4 sec apart. Once during each burst current meter heeling angle, water temperature and time were recorded. The temperature accuracy is 0.1°C and the resolution is .002°C.

A summary of the records considered here is given in Table 2. The first two moorings in this table and CTD Stations 12, 13, 15, and 23 are all within 12 km from each other; hereafter we denote this area as the Deep Site. The first and second moorings in Table 2 are hereafter called the Short Deep and Long Deep Moorings.

CTD Station 12 was made about four hours before the Short Deep mooring record began. CTD Stations 13 and 15 were made during the Short Deep mooring record and CTD Station 23 was made about two days after the Short Deep mooring was recovered and about 18 hours before the Long Deep mooring records began. Thus near-bottom current records are available at the Deep Site several hours after or during the time four CTD Stations were made there.

Progressive vector diagrams for the Short Deep mooring record at 10 m above bottom and for the first two days of the Long Deep mooring record at 15 m are shown in Figure 12. In this figure the beginning of the Long Deep mooring progressive vector diagram was located so that the gap between the two diagrams corresponds to a progressive vector diagram formed from linearly interpolated velocity values inferred from the average of the last 12 hours of the Short Deep record and the average of the first 12 hours of the Long Deep record. Figure 12 approximately indicates when CTD Stations 13 and 15 were made. The positions of CTD Stations 12 and 23 are determined from extrapolated or interpolated velocity data. In the following we assume (1) that the locations of CTD Stations 12 and 23 grossly approximate flow conditions (along or cross-slope flow and weak or strong flow) during the periods of missing data and (2) that the near-bottom currents were horizontally uniform over the area we call the Deep Site.

The current at the times of CTD Stations 12, 13, and 15 was southwesterly (approximately along isobaths in the area (Fig. 1)) and about 15 cm/s ± 5 cm/s (Fig. 12). The BL thicknesses at these three stations were all about 50 m and near-bottom profiles all quite similar (Fig. 9). The current was strongest (about 20 cm/s) on the day Station 13 was made (Fig. 12). The BL at this station was by far the murkiest of all those seen in the *Knorr* 83 data (Table 1).[3] That the BL was murkiest at the

3. Using expressions in Spinrad (1982), a 1 m path length transmissivity of 16%—Station 13 in Table 1—corresponds to a volume concentration of suspended matter of about .78 parts per million. This is quite large by oceanic standards. For comparison, clear sea water has a 1 m path length transmissivity of ~60% and a corresponding volume concentration of suspended matter of ~.03 parts per million.

Table 2. Tabulation of 24-hour Gaussian filtered current meter results except for Deep 6-day record where average of unfiltered velocity data only given. $\overline{KE}$ is the mean kinetic energy per unit mass and KE_f is the kinetic energy per unit mass of the fluctuations.

Station	Location	Depth (m)	BSCM	Height above bottom	Start time	Record length (days)	Average current magnitude (cm/s)	Average current direction °T	$\overline{KE}$	KE_f	Average speed (cm/s)	$\overline{\text{Temp.}}$ (°C)	Temp. std. dev. 10^{-3}°C
Deep	39°55′N 62°23′N	4970	15	10	0420Z 09/29/80	6	9.86	223			10.0		
Deep	39°53′N 62°28′W	4970	13	300	1815Z 10/07/80	230	9.17	269	23.5	32.5	12.7	2.3	9
			15	100		245	8.53	265	56.5	36.3	12.2	2.2	16
			07	15		245	8.86	266	54.3	39.2	12.3	2.2	20
			09	2		245	—	—	—	—	4.6	2.1	20
Middle	40°08′N 62°24′W	4950	14	200	1600Z 10/07/80	174	—	—	—	—	14.1	2.2	12
			11	6		256	4.62	287	10.7	90.2	12.5	2.2	22
Shallow	40°41′N 63°02′W	4500	06	10	1400Z 10/04/80	248	2.23	225	2.5	77.6	11.4	2.2	8

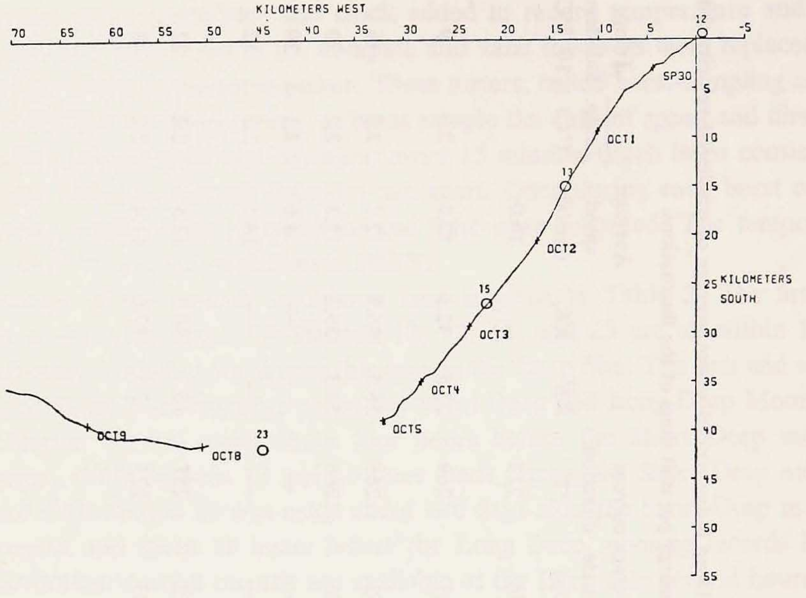

Figure 12. Progressive vector diagrams from the Deep Site obtained at the time of the *Knorr* 83 CTD Survey. Open circles denote when CTD stations 12, 13, 15, and 23 were taken.

time of strongest flow at the Deep Site (Fig. 12, Table 1) is suggestive, but not proof, that bottom sediments go into suspension in the HEBBLE area when the near-bottom currents attain a sustained strength order 20 cm/s.

After 10/01/80 the southwestward flow steadily diminishes and by the beginning of 10/05/80 it is essentially zero with tidal oscillations dominating. Sometime between the release of the Short Deep Mooring (0215 GMT 10/5/80) and the start of the Long Deep Mooring record (1815 GMT 10/7/80) the current picked up. However, the current direction has changed and has a significant cross-slope component (Fig. 12). It seems reasonable that the BL seen at Station 23 was formed several kilometers downslope of the Deep Site during the period of moderately strong, along isobath flows. This BL appears similar to those for Stations 12, 13, and 15 except that its upper ~10 m appears to have been eroded (Fig. 9). Its cap is also more irregular. It is important to note that the BL and its cap for Station 23 represent conditions after a day or so of flow with a significant cross-slope component while for Stations 12, 13, and 15 they represent conditions of fairly uniform along-slope flow. This point is considered again in a later section.

Temperature time series from the four current meters on the Long Deep mooring are shown in Figure 13. The Deep Site was selected for a mooring because it was where we expected the core of the Cold Filament to be on the average. Our intent was to obtain one long record in the BL and one above in the interior. Because we

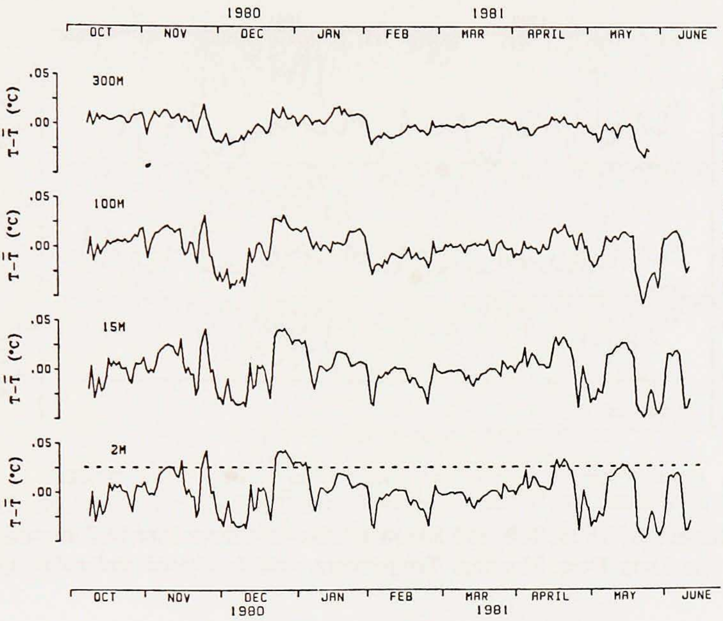

Figure 13. Temperature time series at 2, 15, 100, and 300 m from the Long Deep Mooring. Temperature data were convoluted with a 24 hour Gaussian filter and daily values are plotted. $\bar{T}$ is the record average temperature. See text for dashed line in 2 m record.

were using a new type of current meter, redundancy in vertical positioning was thought to be prudent. Two current meters were placed to be in the BL (2 m and 15 m)[4] and two above (100 m and 300 m). Subsequent analysis of the *Knorr* 83 CTD data, together with the record at 100 m in Figure 13, suggests that the meter at 100 m, while usually above the BL, was often in the BL cap rather than in the interior.

From CTD casts at the Deep Site shortly before launch and 17 km away shortly after recovery (this later data will be reported in another manuscript) we can relate the *in situ* BL current meters temperatures to the BL potential temperature. The dotted line in Figure 13 for the record at 2 m corresponds to $\theta \cong 1.82°C$. We estimate the position of this line to be accurate to about $\pm 5 \times 10^{-3}°C$. If we take the bounding potential temperature isotherm for the Cold Filament to be $\theta = 1.82°C$ (Figs. 2, 6, 7) then the Cold Filament passed over the Deep Site about 86% (+4%, −7%) of the time.

Temperature differences relative to the temperature at 2 m at the Long Deep Mooring are shown in Figure 14. Because the temperature records at 2 and 15 m track so well we conclude that the BL thickness was at least 15 m for the 8-month

4. All height values are above the bottom.

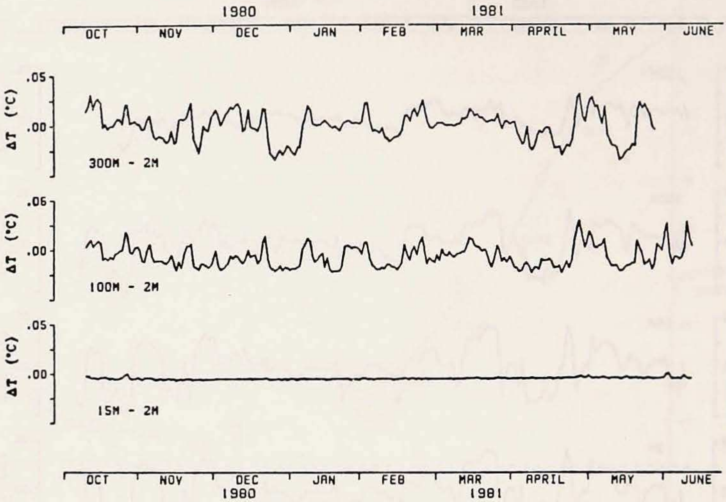

Figure 14. Temperature at 15, 100, and 300 m relative to temperature at 2 m with arbitrary offset from the Long Deep Mooring. Temperature records filtered and subsampled as in Figure 13.

record. The relatively short periods when the BL was stably stratified in October, March, April, May, and June correlate visually with periods of either weak flow or when the current direction abruptly and greatly changed (Fig. 15). Visually many of the temperature changes in the BL (2 and 15 m) correlate with changes in the interior temperature (300 m) (Fig. 13). However, the temperature variability in the BL is generally much larger than above in the interior (Fig. 13 and Table 2). Presumably the greater variability in the BL is due in large part to temporal variability of the core temperature of the Cold Filament and cross-slope migrations of the Cold Filament past the mooring. The *Knorr* 74 CTD data suggest that the core temperature of the Cold Filament varies between 1.75°C and 1.81°C and the *Knorr* 74 and 83 data indicate that it does migrate somewhat cross slope. No attempt is made here to separate the temperature variability in Figure 13 to contributions due to up-stream and cross-stream advective processes. This is the subject of work in progress. The temperature variability at 100 m is intermediate to that in the BL and in the interior; this is presumably due to this current meter having been in the cap region a great fraction of the time.

Velocity vectors from the Long Deep Mooring are shown in Figure 15. No direction data were obtained for the current meter at 2 m. The average speed at this height is underestimated (Table 2) because the rotor frequently stalled. After several months the rotor stall and threshold speeds for this current meter progressively increased to about 5 cm/s and 10 cm/s respectively; its rotor bearings were found to have copious deposits of sediments upon recovery. The rotor on the current meter 13

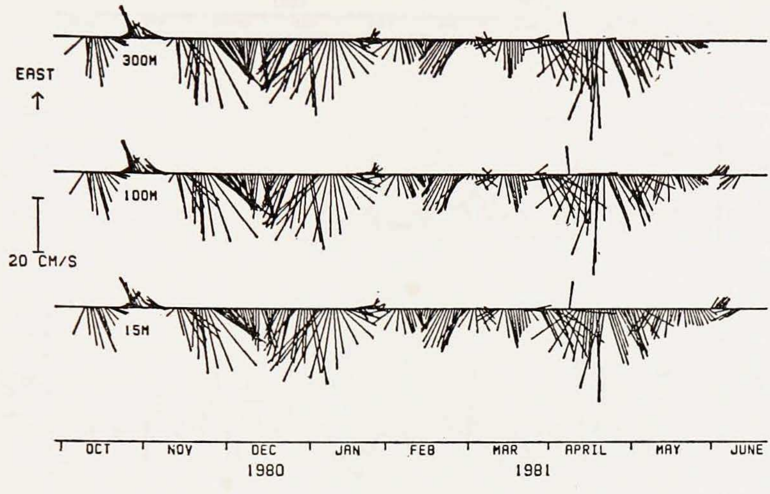

Figure 15. Stick plots for the Long Deep Mooring. Velocity data convoluted with a 24 hour Gaussian and daily values plotted. To form the record at 300 m speed record at 100 m spliced to direction record at 300 m.

at 300 m was broken during launch and no speed record was obtained. To form the velocity record at 300 m in Figure 15 the speed record at 100 m was spliced to the current direction data at 300 m. We think the spliced record to be a reasonable approximation of the current record at 300 m. The magnitude of the average current at 15 m and 100 m differed by only 0.3 cm/s (Table 2). Since more density stratification, and therefore more thermal wind shear, existed between 15 m and 100 m (assuming that the meter at 100 m was usually near the top of the transition region or above it) than between 100 m and 300 m, we expect the velocity shear to be less between 100 m and 300 m than between 15 m and 100 m.

From Figure 15 we see that the near-bottom flow at the Deep Site had a westward bias. Further we see that the Cold Filament is essentially embedded in the overlying or interior flow. It is interesting to note that the average flow at 15 m is a little stronger to west than at 100 m by about 0.3 cm/s (Table 2). While this difference is probably not significant (Bryden, 1976), it is comparable both in magnitude and sense to what is expected by thermal wind provided: (1) that isotherms in the transition region parallel the bottom in a cross-stream sense and (2) that most of the transition region is typically between 15 m and 100 m.

The location of the other sites listed in Table 2, Middle and Shallow, are shown in Figure 5. Time series plots of temperature and velocity for the Middle Site are shown in Figure 16. This site is 28 km east-northeast from the Deep Site; we expected the Filament to pass over it with its core slightly to the south. Not surprisingly many of the temperature and velocity fluctuations in Figure 16 are visually corre-

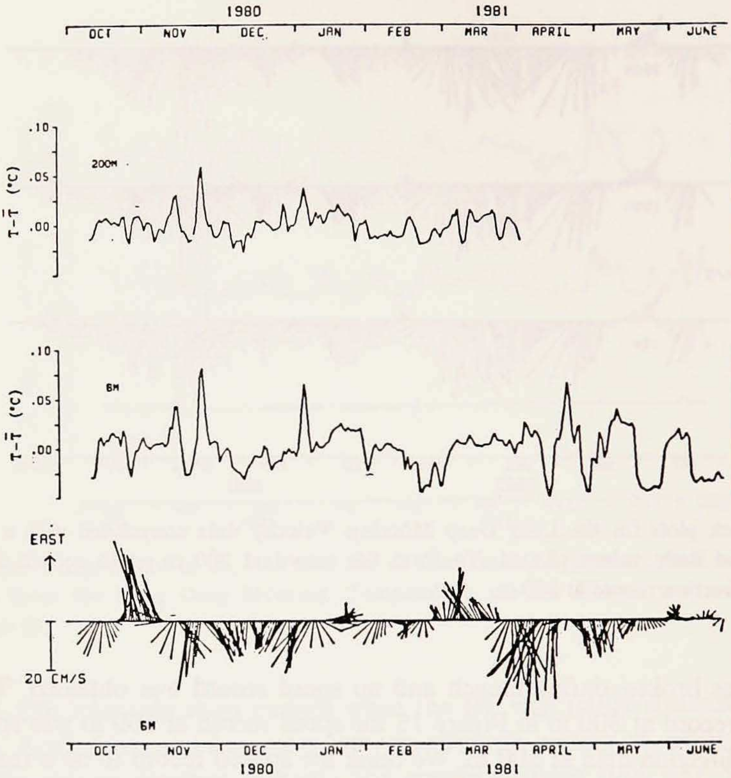

Figure 16. As in Figures 13 and 15 except from Middle Mooring.

lated to those at the Deep Site (Figs. 13, 15). In the same manner as for the Deep Site, we estimate that the Cold Filament passed the Middle Site about 85% (+8%, −7%) of the time. A faulty integrated circuit caused the meter at 200 m to sample at twice the programmed rate resulting in the cassette running out of tape after 176 days. The temperature record at 200 m is long enough, however, to show that, as at the Deep Site, the temperature variability in the BL is larger than in the interior. (Another problem resulted in no direction data from the meter at 200 m.) While the mean flow is weaker at the Middle Site than at the Deep Site (Table 2) the fluctuations are comparable if not somewhat stronger (cf. Figures 15, 16 and KE_f values in Table 2).

Temperature and velocity obtained at 10 m at the Shallow Site are shown in Figure 17. This site is about 100 km northwest (roughly upslope) from the Deep Site. In a zonal sense, the separation of the Shallow Site from both the Deep and Middle Sites is order 50 km. Luyten (1977) found the zonal coherence scale for low frequency fluctuations across the continental rise at 70W to be about 50 km. Thus it is not surprising that there is no apparent visual correlation in the low fre-

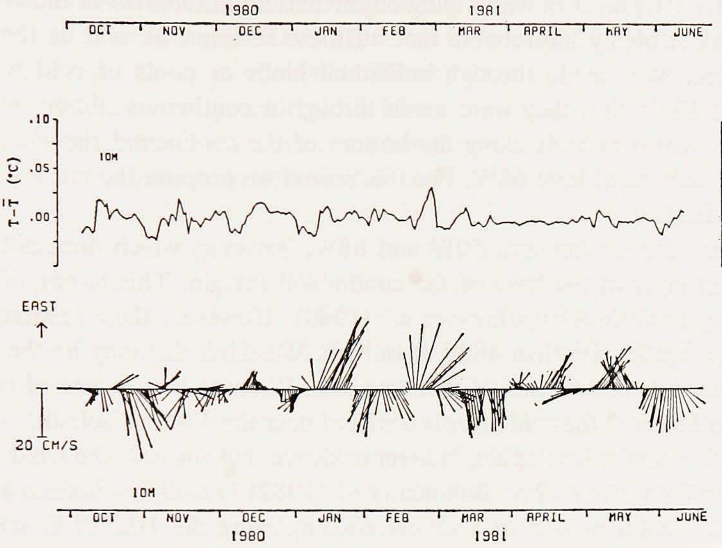

Figure 17. As in Figures 13 and 15 except data from Shallow Mooring.

quency fluctuations at the Shallow Site (Fig. 17) with those at either the Deep Site (Figs. 13, 15) and the Middle Site (Fig. 16). Note that the temperature fluctuations at the Shallow Site BL are much smaller in amplitude than for the BLs at either the Deep or Middle Sites. Apparently the Cold Filament does not often meander upslope to 4500 m depth. While the mean flow at the Shallow Site is weakest, the magnitude of the low frequency fluctuations are of the same order as for the other two sites.

5. Discussion

In examining CTD data from the HEBBLE area (Fig. 1) we found an unexpected feature. A layer of relatively cold ($\theta < 1.82$°C), fresh ($S < 34.984$‰) water was found on the bottom near the base of the continental rise. It was seen on all eight transects reported here (six in the *Knorr* 74 cruise and two in the *Knorr* 83 cruise). Its thickness is about 60 m and its cross isobath width is about 100 km. A similar feature is seen in the same area near the base of the rise in a transect made in 1954 (Fuglister, 1960 or Worthington, 1976). We returned to the area in June, 1981 and again saw it (Weatherly, 1981).

An obvious question is whether a similar feature is seen elsewhere near the base of the continental rise in the western North American Basin. Such a feature is seen eastward of the HEBBLE area at 55W (McCartney *et al.*, 1980) and at 50W (Clarke *et al.*, 1980) and westward at 66W (Fuglister, 1960) and at 68W (Zimmerman, 1971). This last reference is the only one we have found which specifically mentions a cold ($\theta < 1.82°C$) layer of water lying on the bottom at the base of the continental rise. We think it highly improbable that all these sections, as well as the sections presented here, were made through individual blobs or pools of cold water. We think it more likely that they were made through a continuous ribbon or filament of cold water which extends along the bottom of the continental rise near its base from at least 50W to at least 68W. For this reason we propose the name Cold Filament for this feature.

There is one section between 50W and 68W, however, which does not indicate a cold bottom layer at the base of the continental margin. This is one of the two sections along 55W in McCartney *et al.* (1980). However, their sections do not extend further up the rise than 4800 m isobath. We think this may be the reason a cold layer was not seen on one of their sections. We note that in one of the *Knorr* 74 sections in Figure 2 the cold layer is centered near the 4500 m isobath.

There is other nonhydrographic, indirect evidence that suggests the Cold Filament may extend as far west as 72W. Bulfinch *et al.* (1982) in studying bottom sediments along the continental margin in a region encompassing the HEBBLE area to the east, saw coarser particle sizes and efficiently aligned magnetic grains in a 100-200 km wide 400 km long strip along the base of the rise. This strip is roughly centered about the 4900 m isobath. They suggest that strip is due to strong flows at the base of the rise. We, as did Richardson *et al.* (1981), found stronger mean flows at the base of the rise (Table 2) roughly coincident with the location of the Cold Filament.

We expect the Cold Filament to be nearly continuous along the base of the continental rise from at least 50W to at least 72W; however, there are hints of occasional breaks in it. We noted above that in one of the sections in McCartney *et al.* (1980) no Cold Filament appeared. Section 2 in Figure 2 may be interpreted as a filament moving up the rise to about 4500 m depth while a new filament forms at the base of the rise at 5000 m depth. The Deep and Middle site current meter temperature records indicated absence of the Cold Filament about 15% of the time. During these times the Cold Filament may have been pinched off rather than up or down slope of these sites.

A second unexpected result we found is that in the Cold Filament the bottom layer *is* the Cold Filament. That is, the Cold Filament is a distinct layer of water flowing along the bottom with a thickness comparable to that associated with bottom mixed layers. It is interesting to note that Amos *et al.* (1971), in first documenting the existence of bottom mixed layers in the deep ocean, offered two explanations for them: "(1) A homogeneous water mass is flowing beneath another water mass for considerable distance, and intermixing of these two masses is restricted by the stable layer which forms their vertical boundary and (2) A turbulent boundary layer exists at the bottom causing a mixed (homogeneous) layer whose thickness is dependent upon the roughness of the bottom . . . and the magnitude of the current. A similar layer is formed in the atmosphere." Many subsequent investigators have favored the second explanation including one of us (G.W.). However, this does not account for the fact that the BLs in the Cold Filament and often elsewhere in the deep ocean (e.g., Amos *et al.*, 1971; Greenwalt and Gordon, 1978; Armi and D'Asaro, 1980) are clearly "too cold." That is, they are capped with a transition region or thermocline with temperature changes across it much too large to be due to the second explanation. We think that both explanations presented by Amos *et al.* (1971) are required to account for the "too cold" BLs seen in the Cold Filament and elsewhere in the deep ocean. However, we do not imply that BLs in the deep ocean are universally "too cold." Many such layers on the Scotian Rise out of the Cold Filament and elsewhere in the deep ocean (e.g., Armi and Millard, 1976) clearly are not. Nonetheless "too cold" bottom layers, while not ubiquitous in the deep ocean, are common at least in the western North Atlantic.

The eight month temperature and velocity data obtained at the Deep Site show that the Cold Filament passed this site about 85% of the time and it flows equatorward. The dissolved silicate content of waters in and surrounding the Cold Filament are typical for the North American Basin although some northern source water is sometimes seen (Richardson *et al.*, 1981). That is, the water flowing equatorward at the base of the Scotian Rise does not appear typically to be cold, deep, low silicate, Labrador Basin water which has found its way into the North American Basin by flowing around the Newfoundland Ridge. This is further substantiated by the θ-S properties of the deep water at the base of the Scotian Rise (Fig. 11). Thus it seems likely that the equatorward flowing water at the Deep Site is the return flow of deep poleward flow on the Sohm Abyssal Plain east of the HEBBLE area.

The eight month current records further up the rise, i.e., the Middle and Shallow Mooring, also show equatorward flow (Table 2). The Middle mooring, from its temperature data (Figure 12) extended into the Cold Filament; however, it is upslope of where we expect the core of the Cold Filament to be on the mean. Its eight month average velocity is about 50% that seen at the Deep Mooring. At the Deep and Middle Moorings the average flow (Table 2) was approximately along isobaths (Fig. 5) and directed toward the equator. We expected the average flow to be directed more toward the southwest rather than toward the west. The near-bottom flow direction at these two sites may reflect constraints imposed by upstream topography. Along 62W a broad (~60 km), low (~50 m) ridge is found between 40 and 41N (Fig. 5).

The mean flow magnitude at the Shallow Mooring is about 25% that at the Deep site. However, the low frequency events seen there are comparable in strength to those seen at the Middle and Deep sites. The average current direction at the Shallow site was southwestward and approximately along the trend of the local isobaths. Because the strength of the low frequency events, which from Figure 15 can be seen to be oriented primarily east-west, is so much greater than the record mean flow, the average current direction and magnitude may not be significant. However, the same data in Figure 15 presented in progressive vector form (not shown here) show a clear southwestward trend to the currents there. The low frequency east-west events appear to be imposed on a weak (~2 cm/s) southwestward mean flow.

Based on our and others' data we have postulated that the Cold Filament flows from about 50W to at least 72W equatorward, embedded in the overlying water, along the base of the continental rise. We suspect it is formed at the base of the continental rise near 50W by the confluence of poleward flowing bottom layers on the abyssal plain in the North American Basin and is part of a larger (at least thicker) circulation pattern which may be a western boundary undercurrent associated with a southern water source as in Stommel *et al.* (1958) or an eddy driven deep flow seen in the numerical models of Holland and Rhines (1980). Taking for representative width, thickness and velocity values as, respectively, 100 km, 60 m and .09 m/s, the volume transport of the Cold Filament in the HEBBLE area is about 0.5×10^6 m^3/s. That the Cold Filament maintains its identity as it flows is probably due to the large density gradient capping it. Estimates of the Richardson number for the cap region above the Cold Filament made using σ_5 profiles (e.g., Fig. 8) to estimate the density contrast and either the thermal wind relations or current meter data to estimate the velocity contrast together with a representative thickness of the transition region of 100 m (see Table 1) give values order 10^3. This suggests that shear generated turbulence in the Cold Filament cannot penetrate effectively into the overlying fluid to mix Cold Filament water with overlying water. Thus the Cold Filament may flow considerable distances with little intermixing with water above it.

In contrast to Pak and Zaneveld (1982) who considered the *Knorr* 74 data we found the thickness of the *Knorr* 83 BLs determined from θ and transmissivity profiles to be usually the same. (We found the same for the BL cap; however, they do not consider in detail the BL cap.) This discrepancy may be due to the subjective manner used to determine thicknesses of these layers. However, these differences may be real. During the time of the *Knorr* 83 survey the near-bottom currents appear to have been somewhat weaker than during the *Knorr* 74 survey. Richardson *et al.* (1981) and Bird *et al.* (1982) show that for about a week during the *Knorr* 74 survey near-bottom currents near the base of rise were relatively strong (20-40 cm/s). Data presented here show that in the same general area during the *Knorr* 83 cruise the strongest recorded flow was only about 20 cm/s and comparatively short in duration (Fig. 12). During this time the murkiest BL (Table 1, Station 13) was observed. Pak and Zaneveld observed more, comparably murky BL in the *Knorr* 74 survey. With results presented here we have suggested that sediments may be notably eroded when near-bottom currents attain a magnitude order 20 cm/s. About two-thirds of the six transmissivity sections for the *Knorr* 74 cruise show a rough similarity with the corresponding θ-sections (cf. Figs. 3 and 4). Both for the *Knorr* 83 cruise show a stronger similarity (cf. Figs. 6 and 7). We think it likely that differences in BL transmissivity conclusions inferred from the surveys are partly due to differing flow conditions. During periods of varying strong flows which result in appreciable and varying sediment erosion there is no *a priori* reason to expect near-bottom transmissivity profiles or sections to have a one-to-one correspondence to θ-profiles or sections.

The thickness of the transition region capping the BLs was found to be comparable to the thickness of the BLs (Table 1). This was unexpected. One possible explanation for relatively thick transition regions is salt fingering. Using the profile shown in Figure 8 as an example, the BL is colder and fresher than the water above in the interior. The density ratio $R \equiv \alpha \, \Delta \, \theta / \beta \, \Delta \, S$ (Schmitt, 1979) across the BL cap is about 1.2. Here we have taken $\Delta\theta = .035°C$, $\alpha = 1.95 \times 10^{-4}$ (°C)$^{-1}$, $\Delta S = .0075‰$, and $\beta = 7.37 \times 10^{-4}$ (‰)$^{-1}$. An effective diffusion coefficient for salt fingering for $R = 1.2$ is about 10^{-3} m^2/s (Schmitt, 1981). The average cap thickness for the Cold Filament is about 100 m (Table 1). Thus a diffusive time scale T_D is $T_D \sim (100 \text{ m})^2/10^{-3} \text{ m}^2/\text{s} \sim 100$ days. If a thin cap is formed presumably where the Cold Filament is formed south of the Newfoundland Ridge, and advects 1000 km to the HEBBLE area at 9 cm/s (Table 2) in time T_a, then $T_a \sim 1000$ km/9cm/s ~ 110 days. Since $T_D \sim T_a$ it is not inconsistent that thick BL caps in the HEBBLE area could be due to salt fingering.

Another and we expect more probable explanation for thick BL caps, and thicker Cold Filament BL caps, is boundary layer separation from the bottom. When the near-bottom flow along the continental rise has a significant and persistent cross-slope component it seems reasonable that at those times the BL may separate from the bottom after it has progressed some (unknown) distance cross slope. From the current meter records shown here it is apparent that cross-slope advection of BLs on the Scotian Rise is not uncommon. After separation the layer would become part of the transition region above the new BL beneath it.

The presence of the Cold Filament may enhance BL separation particularly near its upslope and downslope edges. The θ and transmissivity profiles above the BL and below 300 m for Station 16—which is upslope of the core, but in the Cold Filament—show several relatively murky, quasi-isothermal layers over each other (Fig. 10). It seems likely that they are relic BLs which separated from the bottom. The layer centered about 175 m at this station appears to extend further upslope at about the same height above bottom—cf. Stations 17 and 18 profiles in Figure 9. Suggestions of separated BLs in the transition region are apparent in many of the Cold Filament profiles in Figure 9.

Weatherly and Lonsdale (in preparation), in analyzing CTD/transmissometer data obtained in a Deep Tow survey of the HEBBLE area in June, 1981, show results which suggest the upslope edge of the Cold Filament is sharp or frontlike rather than gradual as indicated in Figures 2, 6, 7. They show that at the upslope edge of the Cold Filament the temperature changes by about $\sim .040°C$ in 300 m horizontal distance. Their data, obtained in a period of weak cross-slope flow, also show what appears to be separated BLs to be common near the front. This suggests to us that if there is a differential cross-slope velocity in the BLs on either edge of the front that the lighter BL outside the Cold Filament will tend to separate from the bottom at the front and override the BL in the Cold Filament rather than mix horizontally with it.

While we expect BL separation not to be uncommon in the HEBBLE area in periods of prolonged cross-isobath flow and at the edges of the Cold Filament, we do not expect it to be common in periods of prolonged long-isobath flow at least away from the edges of the Cold Filament. The *Knorr* 83 Deep Site profiles 12, 13, and 15 were obtained over an interval when the flow was rather steady and along isobath (Fig. 12). The BL thicknesses are the same and the structure of the near-bottom profiles similar. That the BL for Station 13 is thermally stratified may be due to it being an evolving BL (the bottom flow was peaking then (Fig. 12)) and very sediment-laden. Buoyancy effects associated with the latter may have hindered vertical mixing in the BL. The profile for Station 23 shows a BL and cap similar to that for Stations 12, 13, and 15. Its differences, an eroded appearance at the top of the BL and a jagged structure to the cap, may be due to cross-slope advective processes occurring during the preceding short period of weak cross-slope flow. That the BLs seen at the Deep Site during the period of long-slope flow in Figure 12 are so similar suggests that BL conditions may have been rather uniform over several tens of km in an upstream sense during this period. Station 16 was taken about 18 km upslope of the Deep Site and its BL thickness is comparable to those at Stations 12, 13, and 15 at the Deep Site. Thus, the BL may also have been uniform over cross-stream spatial scales of about order ten km during this period of long isobath flow. This suggests that a z,t or so-called one-dimensional BL model similar to that used in Weatherly and Martin (1978) may be suitable for describing BLs in the HEBBLE area (excluding regions at the edge of the Cold Filament) in conditions of sustained long isobath flow.

Acknowledgments. We thank R. Zaneveld and H. Pak for making the *Knorr* 74 CTD data available, and J. Szelag and R. Millard, Jr. for their roles in obtaining and processing respectively the *Knorr* 83 CTD data. Especial appreciation is extended to D. Hunley and W. Sturges III for making the current meters (the BSCMs) a reality in a few months time. R. Harkema is thanked for his efforts in the data processing and M. LaBarge and P. Arnold, for typing the manuscript. This work was done as part of the ONR High Energy Benthic Boundary Layer Experiments (HEBBLE) Program and was supported by Contract N00014-75-C-0201 with the Office of Naval Research.

REFERENCES

Amos, A. F., A. L. Gordon and E. D. Schneider. 1971. Water masses and circulation patterns in the region of the Blake-Bahama Outer Ridge. Deep-Sea Res., *18,* 145–165.

Armi, L. and E. D'Asaro. 1980. Flow structures of the benthic ocean. J. Geophys. Res., *85,* 469–484.

Armi, L. and R. C. Millard, Jr. 1976. The bottom boundary layer of the deep ocean. J. Geophys. Res., *81,* 4983–4990.

Bird, A. A., G. L. Weatherly and M. Wimbush. 1982. A study of the bottom boundary layer over the eastward scarp of the Bermuda Rise. J. Geophys. Res., *87,* 7941–7954.

Bryden, H. L. 1976. Horizontal advection of temperature for low frequency motions. Deep-Sea Res., *23,* 1165–1174.

Bulfinch, D. L., M. T. Ledbetter, B. B. Ellword and W. L. Balsam. 1982. The high velocity core of the Western Boundary Undercurrent at the base of the U.S. continental rise. Science, *215,* 970–973.

Clarke, A. A., H. Hill, R. F. Reiniger and B. A. Warren. 1980. Current system south and east of the Grand Banks of Newfoundland. J. Phys. Oceanogr., *10,* 25–65.

Fuglister, F. C. 1960. Atlantic Ocean atlas of temperature and salinity profiles and data from the International Geophysical Year of 1957-1958. Woods Hole Oceanographic Institution Atlas Series, *1,* 209 pp.

Greenwalt, D. and C. M. Gordon. 1978. Short term variability in the bottom boundary layer of the deep ocean. J. Geophys. Res., *83,* 4713–4716.

Holland, W. R. and P. B. Rhines. 1980. An example of eddy-induced ocean circulation. J. Phys. Oceanogr., *10,* 1010–1031.

Hollister, C. D., A. R. M. Nowell and J. D. Smith. 1980. The Third Annual Report of the High Energy Benthic Boundary Layer Experiment, WHOI Ref. 80-32.

Kelley, E. A., G. L. Weatherly and J. C. Evans. 1982. Correlation between surface Gulf Stream and bottom flow near 5000 meters depth. J. Phys. Oceanogr., (in press).

Luyten, J. R. 1977. Scales of motion in the deep Gulf Stream across the continental rise. J. Mar. Res., *35,* 49–74.

McCartney, M. S., L. V. Worthington and M. E. Raymer. 1980. Anomalous water mass distribution at 55W in the North Atlantic in 1977. J. Mar. Res., *38,* 141–171.

Pak, H. and J. R. V. Zaneveld. 1982. Observations of bottom mixed layers and nepheloid layers off Nova Scotia, (submitted).

Richardson, M. J., M. Wimbush and L. Mayer. 1981. Exceptionally strong near-bottom flows on the continental rise of Nova Scotia. Science, *213,* 887–888.

Schmitt, R. W., Jr. 1979. The growth rate of super-critical salt fingers. Deep-Sea Res., *26A,* 23–40.

Schmitt, R. W., Jr., 1981. Form of the temperature-salinity relationship in the Central Water: evidence for double-diffusive mixing. J. Phys. Oceanogr., *11,* 1015–1026.

Spinrad, R. W. 1982. Characteristics of suspended sediments in the High Energy Benthic Boundary Layer Experiments, Ph.D. thesis, Oregon State University.

Stommel, H., A. B. Aarons and A. J. Faller. 1958. Some examples of stationary planetary flow patterns in bounded basins. Tellus, *10,* 179–187.

Weatherly, G. L. 1981. A Deep Tow survey in the HEBBLE area. Trans. Am. Geophys. Union, *62,* (Abstract), 898.

Weatherly, G. L. and P. J. Martin, Jr. 1978. On the structure and dynamics of the oceanic bottom boundary layer. J. Phys. Oceanogr., *8,* 557–570.

Weatherly, G. L. and E. A. Kelley, Jr. 1981. An analysis of hydrographic data from *Knorr* Cruise 74 in HEBBLE area, September-October 1979. Florida State University Technical Report.

Weatherly, G. L., E. A. Kelley, Jr. and R. Harkema. 1981. An analysis of hydrographic data from *Knorr* Cruise 83 in HEBBLE area, October 1980. Florida State University Technical Report.

Worthington, L. V., 1976. On the North Atlantic circulation. The Johns Hopkins Oceanographic Studies, *6,* 110 pp.

Wright, W. R. and L. V. Worthington. 1970. The water masses of the North Atlantic Ocean; a volumetric census of temperature and salinity. Serial Atlas of the Marine Environment, Folio 19, American Geophysical Society, New York, 8 pp. and 7 plates.

Received: *29 April, 1982;* revised: *24 June, 1982.*